

論文 / 著書情報  
Article / Book Information

題目(和文)	高いInGa組成を有するCu(InGa)Se <sub>2</sub> 太陽電池の高効率化に関する研究
Title(English)	Study of High Efficiency Cu(InGa)Se <sub>2</sub> Solar Cells with High Ga Content
著者(和文)	平井義晃
Author(English)	Yoshiaki Hirai
出典(和文)	学位:博士(工学), 学位授与機関:東京工業大学, 報告番号:甲第9783号, 授与年月日:2015年3月26日, 学位の種別:課程博士, 審査員:山田 明,小長井 誠,岩本 光正,中川 茂樹,宮島 晋介,櫛屋 勝巳
Citation(English)	Degree:, Conferring organization: Tokyo Institute of Technology, Report number:甲第9783号, Conferred date:2015/3/26, Degree Type:Course doctor, Examiner:,,,,,
学位種別(和文)	博士論文
Category(English)	Doctoral Thesis
種別(和文)	要約
Type(English)	Outline

# Study of High Efficiency Cu(InGa)Se<sub>2</sub> Solar Cells with High Ga Content

Presented by Yoshiaki Hirai and Directed by Professor Akira Yamada

Department of Physical Electronics, Graduate School of Science and Engineering,  
Tokyo Institute of Technology

## 1. Introduction

An increase of World's population has increased World's energy consumption. This situation causes insufficiency of energy resources because the fossil fuel that is finite is main energy resource. Moreover, consuming the fossil fuel causes large amount of emissions of CO<sub>2</sub>, which is one of the greenhouse gases. Therefore, renewable energy sources have attracted great attention as alternative to fossil fuels. In such a situation, solar cells has been paid attention because these have some unique advantages, e.g., unlimited energy source, no moving part, and short energy payback time. On the other hand, solar cells have issues, e.g., low energy density of the sunlight and high cost. In order to solve these issues, increasing efficiency of solar cells must be required, keeping their cost low. As a material fulfills these requirements, Cu(InGa)Se<sub>2</sub> (CIGS) is promising.

CIGS has the high absorption coefficient, which contributes to low cost fabrication due to reducing thickness of the absorber layer. Moreover, CIGS can increase bandgap from approximately 1.0 to 1.7 eV by increasing a ratio of Ga/(In + Ga) from 0 to 100%. Therefore, high efficiency CIGS solar cells are expected for bandgap of 1.4 eV, accordingly a

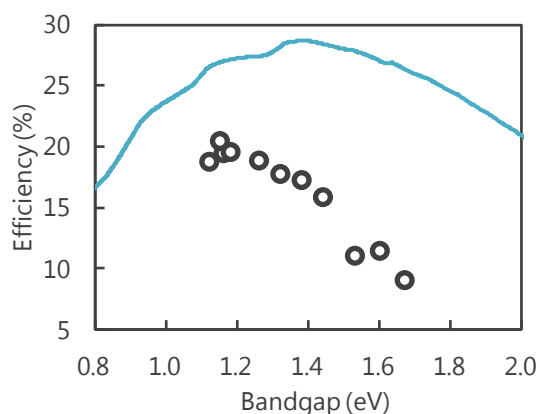


Fig. 1. Theoretical and experimental bandgap dependence of CIGS solar cells efficiency. Blue line shows theoretical efficiency. Black outlined dots shows experimental results reported by NREL group<sup>[5]</sup>.

Ga content of 70%, because of the matching of sunlight spectrum. However, efficiency decreases with increasing Ga content as shown in Fig. 1, although CIGS solar cells with a efficiency of above 20% were obtained by several groups in the case of a bandgap of approximately 1.15 eV,<sup>[1-4]</sup> accordingly, a Ga content of approximately 30%. In order to increase efficiency of CIGS solar cells with high Ga content, this thesis focused both on an electron barrier near the surface of CIGS and on the recombination process at CdS/CIGS interface.

## 2. Effects of Ga Content on CIGS Solar Cell Performance

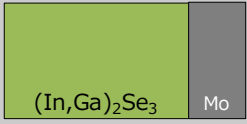

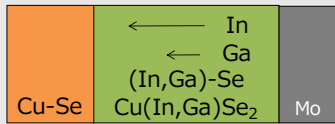
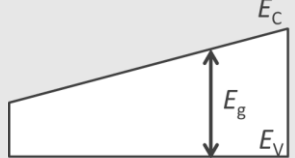
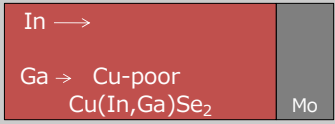
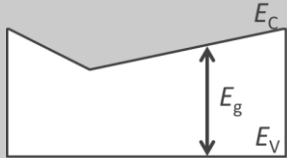
### 2-1. Change of CIGS Absorber

High-quality CIGS thin films have been generally prepared by using a three-stage method and a type of multisource vacuum evaporation system.<sup>[6-8]</sup> This method contributes to the growth of CIGS with a notch shaped conduction band profile. The mechanism of forming the conduction band profile was shown in Table I. The conduction band profile is attributed to the low diffusivity of Ga atoms, compared with In atoms, on the growing surface<sup>[9]</sup> and the constant valence

band level regardless of Ga content.<sup>[10]</sup> Conduction band grading on the Mo back contact side allows us to efficiently collect electrons in a p-type absorber, resulting in an increase of current density. Conduction band grading on the surface side allows us to repel electrons from the CdS/CIGS heterointerface, resulting in an increase of open circuit voltage.

In the case of CIGS with a high Ga content, the notch becomes very deep because of Ga profile as shown in Fig. 2. This deep notch obstructs the minority carrier collection in the absorber. Electrons accumulated at the notch cause carrier recombination in the absorber, subsequently degrading device performance.

Table. I. Mechanism of forming conduction band profile in three stage method.

Process	Status of Film	Band profile
<b>First stage</b> (In, Ga and Se fluxes are irradiated.)	Precursor of $(\text{InGa})_2\text{Se}_3$ forms.  In →  Ga → Se →	Flat band profile is formed.  
<b>Second stage</b> (Cu and Se fluxes are irradiated.)	Cu(InGa)Se <sub>2</sub> is formed by Cu diffusion from surface. Liquid phase of Cu-Se increases grain size of Cu-rich Cu(InGa)Se <sub>2</sub> .  Cu →  Se →	In and Ga content around surface and back surface of Cu(InGa)Se <sub>2</sub> , respectively, increases because of the low diffusivity of Ga atoms compared to In atoms.  
<b>Third stage</b> (In, Ga and Se fluxes are irradiated.)	Cu-poor Cu(InGa)Se <sub>2</sub> forms, which Cu content is in the range of 0.7-0.9.  In →  Ga → Se →	Ga content around surface increases because of the low diffusivity of Ga atoms as with the second stage.  

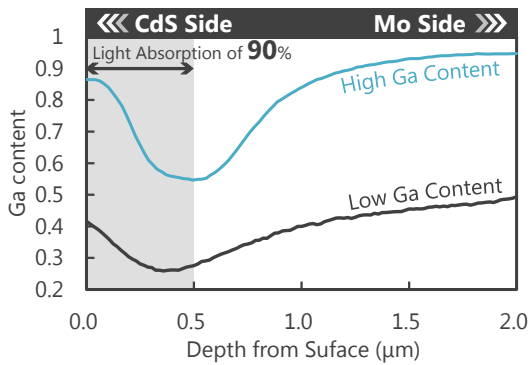


Fig. 2. Profile of Ga content in CIGS Thin-films. Blue and Orange line shows Ga profile of CIGS with Ga content of 30 and 70%, respectively. Ga profile was determined by SIMS measurement from back contact side. Gray-colored area shows the region where 90% of light absorption in the whole CIGS layer is absorbed.

## 2-2. Change of CdS/CIGS Interface

A typical pn junction interface of CIGS solar cells is composed of n-type CdS and p-type CIGS. CdS prepared by CBD forms epitaxial interface with CIGS in the case of a Ga content of approximately 30% owing to a low lattice mismatch of 1.5%. In the case of a Ga content of above 30%, however, the lattice constant of CIGS decreases with increasing Ga content, resulting in formation of a defective CdS/CIGS interface. In addition, change of the conduction band offset (CBO) at CdS/CIGS heterointerface due to an increase of Ga content affects interface recombination rate.

Figure 3 shows the conduction band alignment of typical CIGS solar cells. Conduction band minimum (CBM) of CIGS increases with increasing Ga content because valence band maximum (VBM) of CIGS

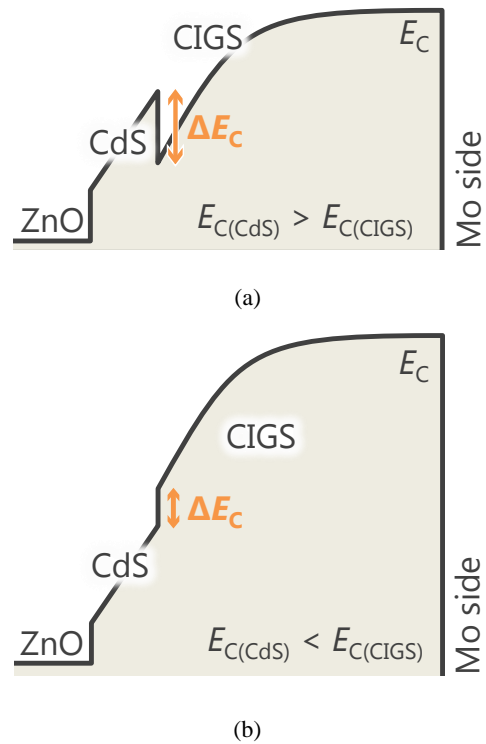


Fig. 3. Conduction band alignment of CIGS solar cells with CdS buffer layer and ZnO TCO layer. When CBM of  $\text{Cu}(\text{InGa})\text{Se}_2$  lower and higher than that of CdS, CdS/CIGS heterointerface is (a) spike and (b) cliff interface, respectively.

change slightly regardless of Ga content. CBM of CIGS is lower than that of CdS when Ga content is less than 40%, resulting in a spike CdS/CIGS heterointerface as shown in Fig. 3(a). On the other hands, CBM of CIGS is higher than that of CdS when Ga content is more than 40%, resulting in a cliff CdS/CIGS heterointerface as shown in Fig. 3(b). Electrons injected from TCO layer by forward bias voltage are easy to reach the cliff interface, consequently, the cliff interface causes the recombination between electrons in CdS and holes in CIGS at the CdS/CIGS heterointerface.<sup>[11]</sup>

### 3. Modification of Preparation Method for CIGS thin-films with High Ga content

#### 3-1. Five-Stage Method<sup>[12]</sup>

In order to suppress separation of In and Ga atoms in CIGS thin-films, it is needed to shorten diffusion length of these atoms. Therefore, a five-stage method, modified three-stage method, was carried out.

CIGS thin films were prepared by the five-stage method on to Mo-coated soda-lime glass substrate. Figure 4 shows the substrate temperature profile during the five-stage method. In the first stage, In, Ga and Se fluxes were irradiated to the substrate which was kept at a temperature of 380 °C for 15 min. Then, the substrate temperature increased up to 520 °C, subsequently Cu and Se fluxes were irradiated during the second stage. After observation of the temperature drop due to an increase of Cu composition, In, Ga, and Se fluxes were irradiated for 25 min. at same temperature during third stage. Again, Cu and Se fluxes were irradiated until observation of the temperature drop during fourth stage, finally In, Ga, and Se atoms were deposited in order to control the film content.

As a result, a profile of Ga content was changed, as shown in Fig. 5. The depth of the notch in the CIGS thin-film prepared by the three-stage and the five-stage method corresponds to approximately 0.23 and 0.11 eV, respectively. This result indicates that the five-stage method is effective in control of increasing the depth of the notch owing to excessive Ga separation in CIGS thin-films

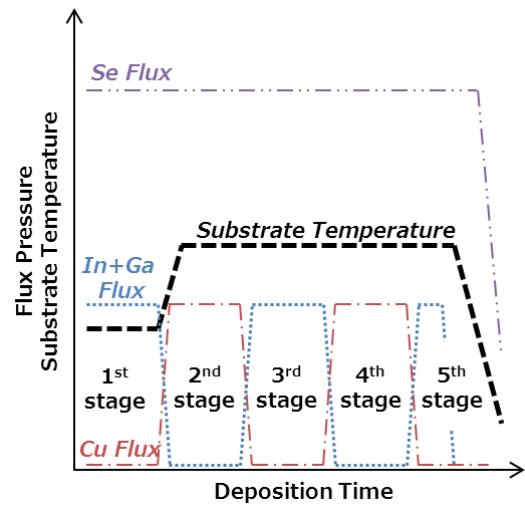


Fig. 4. Substrate temperature profile.

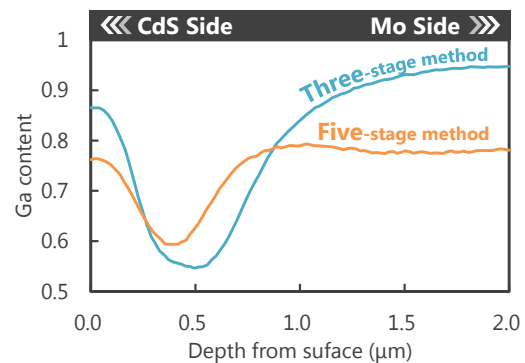


Fig. 5. Profile of Ga content in CIGS thin-films with high Ga content.

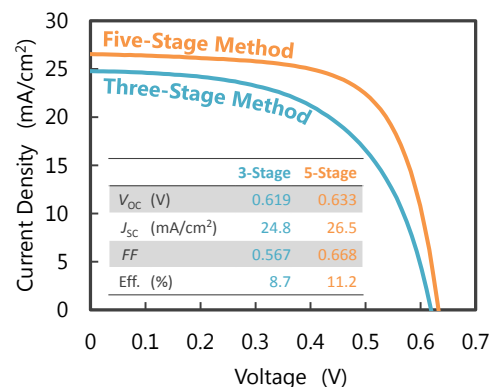


Fig. 6. *J-V* characteristics of CIGS solar cells with high Ga content prepared by three-stage and five-stage method.

with high Ga content. Decreasing the depth of the notch yields improvement in bias voltage dependence of minority carrier collection. As a result, improvement of solar cell characteristic was obtained, especially FF, as shown in Fig. 6. However, an increase of  $V_{OC}$  was small. One should consider the possibility that a flat conduction band profile, which causes carrier recombination easily, at the back contact side is formed by uniform Ga distribution.

### 3-1. High Temperature Preparation

In order to form graded conduction band profile at the Mo back contact side while keeping the shallow notch, promotion of Ga diffusion during the three-stage method by raising preparation temperature was attempted.

CIGS films were prepared by the three-stage method onto Mo-coated Glass with a strain point of 645 °C, as shown in Fig. 7. In the first stage, In, Ga and Se fluxes were irradiated to the substrate which was kept at a temperature of 380 °C for 40 min. Then, the substrate temperature increased up to 640 °C, different depending on experiment. Then, Cu and Se fluxes were irradiated during the second stage. After observation of the temperature drop due to an increase of Cu composition, In, Ga, and Se fluxes were irradiated in order to control the film content. During preparation, Se flux increased up to  $1.0 \times 10^{-2}$  Pa to suppress decomposition of CIGS due to raising substrate temperature.

As a result, a profile of Ga content was changed, as shown in Fig. 8. As shown in this figure, first, suppressing the separation of Ga

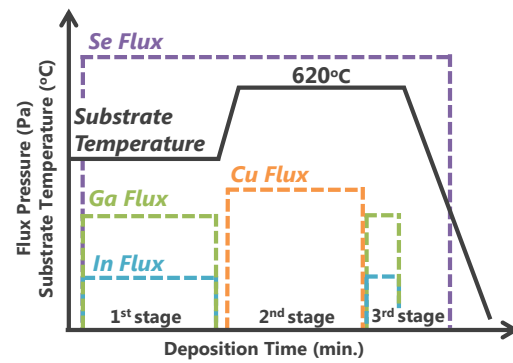


Fig. 7. Substrate temperature profile.

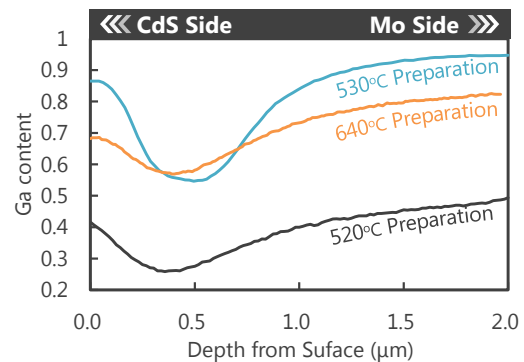


Fig. 8. Profile of Ga content in CIGS thin-films.

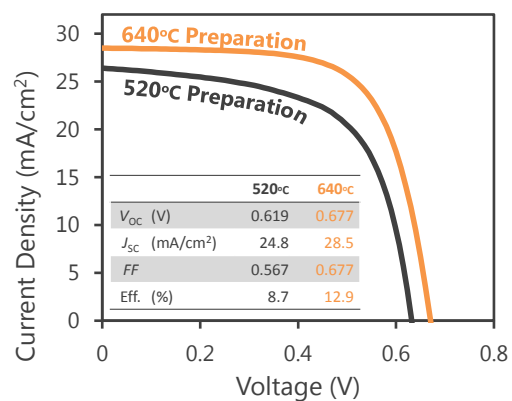


Fig. 9. Profile of Ga content in CIGS thin-films.

atoms succeeds, corresponding to a decrease of notch depth from approximately 0.23 to 0.07 eV. Second, the graded profile of Ga content around Mo contact side in the CIGS layer

succeeds. As a result of these improvements in the profile of Ga content, the profile in the CIGS with high Ga content prepared at high temperature become similar to the profile in the CIGS with low Ga content. This improvement of conduction band profile yielded an increase of efficiency up to 12.9%, as shown in Fig. 9. However,  $V_{OC}$  was still lower than the expectation, although it increased as compared to the case of the typical three-stage method.

#### 4. Theoretical Analysis of High Efficiency CIGS Solar Cells with High Ga Content<sup>[13]</sup>

To disclose effects of the conduction band profile on solar cell performance, numerical evaluation was carried out. Effects of the conduction band profile were evaluated numerically at the condition that an average bandgap of CIGS layers were 1.4 eV. Simultaneously, because the CdS/CIGS interface recombination was taken into account

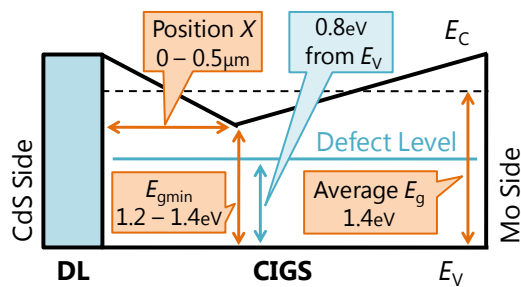


Fig. 10. Device structure of CIGS solar cells used in this simulation for evaluating effect of conduction band profile. Left side and right side is CdS buffer layer and Mo back contact, although there layer are omitted form this figure. Blue solid and black dashed line in CIGS layer represents position of defect and average bandgap of 1.4 eV.

in this numerical evaluation, effects of suppressing the interface recombination on solar cell performance were also evaluated by focusing on the valence band offset ( $\Delta E_V$ ) at the CdS/CIGS interface.

#### 4-1. Effects of Conduction Band Profile

An optimum conduction band of CIGS was evaluated under the condition that an average bandgap of 1.4 eV was constant. The conduction band profile was changed by varying the minimum bandgap  $E_{gmin}$  and its position  $X$ , as shown in Fig 10. It was assumed that the bandgap and electron affinity of a defective layer (DL) were the same as those of the CIGS surface,  $E_{gmin}$  was varied from 1.20 to 1.40 eV, and  $X$  was varied from 0 to 0.5  $\mu\text{m}$ .

Efficiency distributed as shown in Fig. 11. From this distribution, a maximum efficiency of 17.0% was obtained at  $X = 0.05 \mu\text{m}$  and  $E_{gmin} = 1.23 \text{ eV}$ . This efficiency was much

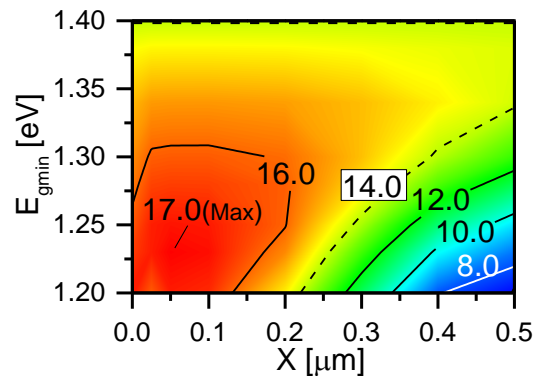


Fig. 11. Distribution of Efficiency against  $E_{gmin}$  and  $X$ . Vertical and horizontal axes represents  $X$  and  $E_{gmin}$ , respectively. Red and blue region shows relatively high and low values, respectively. Solid lines represent contour values. Dashed line represents contour values for CIGS with the flat conduction band profile.

lower than the expectation because of the trade-off in the distribution between FF and  $V_{oc}$ .

#### 4-1. Effects of $\Delta E_V$ Formation

In order to suppress the interface recombination at CdS/CIGS, the formation of the valence band offset ( $\Delta E_V$ ) at the surface of the CIGS layer seems to be effective in repelling holes from CdS/CIGS interface. The effects of the  $\Delta E_V$  at the CdS/CIGS interface were evaluated by incorporating a surface layer (SL) into the DL/CIGS interface, as shown in Fig. 12. The bandgap of CIGS with a flat conduction band, i.e., with a uniform depth profile of Ga content, was varied from 1.05 to 1.6 eV with the defect level fixing at a peak energy of 0.8 eV from  $E_V$ . At the same time, each bandgap of SL and DL was varied, maintaining the same electron affinity as the CIGS surface and the same bandgap as CIGS plus the value of  $\Delta E_V$ . In this calculation, the effect of the  $\Delta E_V$  on solar cell

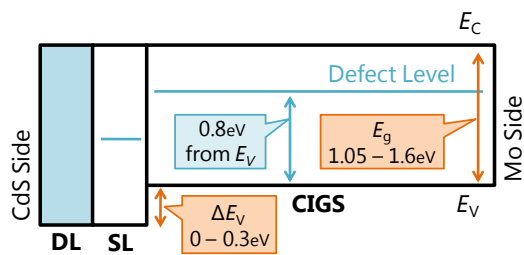


Fig. 12. Device structure of CIGS solar cells used in this simulation for evaluating effect of the  $\Delta E_V$ . Left side and right side is CdS buffer layer and Mo back contact, although there layer are omitted from this figure. Blue solid represents position of defect level.

performance was investigated by changing the  $\Delta E_V$  from 0 to 0.3 eV.

Figure 13 shows the relation between the bandgap of the CIGS layer with the flat conduction band and  $\Delta E_V$ . From this figure, when  $\Delta E_V$  is small, efficiency increases with increasing  $\Delta E_V$ . Moreover, a higher efficiency is calculated in the case of  $E_{gmin} = 1.15$  eV. Subsequently, efficiency decreases with increasing bandgap of CIGS beyond 1.15 eV. This tendency is very consistent with the experimental result reported by the NREL group,<sup>[5]</sup> shown as black dots in Fig. 13, particularly for  $\Delta E_V = 0.05$  eV. When  $\Delta E_V$  increases, the efficiency of wide-bandgap CIGS increases monotonically, although that of narrow-bandgap CIGS increases slightly. As a result, by increasing  $\Delta E_V$  up to 0.3 eV, the highest efficiency was obtained at the a bandgap in the CIGS layer of approximately 1.35 eV, which is close to the estimated bandgap for obtaining the highest efficiency owing to the matching of the sunlight spectrum.

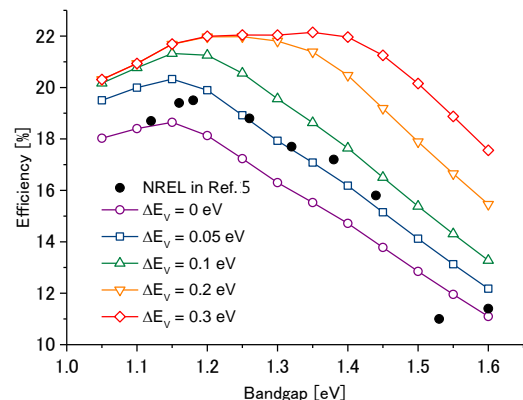


Fig. 13. Relation between bandgap of CIGS layer with flat conduction band and  $\Delta E_V$ . Black dots represent experimental result reported by NREL group.<sup>[5]</sup>

## 5. Improvement of CdS/CIGS Interface Incorporating Surface Layer with $\Delta E_V$

Taking the result of numerical evaluation into account, it was evaluated the effect of  $\Delta E_V$  at the CdS/CIGS interface on solar cell performance, especially  $V_{OC}$ . In this study, incorporation of ZnSe thin-films into the CdS/CIGS interface was conducted. At first, ZnSe thin-film was deposited onto CuInSe<sub>2</sub> by ALD-like process in the chamber which is equipped with not only Cu, In, Ga, and Se but Zn Kunudsen cell in order to confirm the formation of ZnSe thin-films and investigate the deposition rate of ZnSe thin-films. Then, it was found that the layer by layer deposition of ZnSe thin-films was conducted. As a result of incorporation ZnSe thin-film into the typical solar cell structure, a  $V_{OC}$  of 0.792 V was obtained by increasing the ZnSe thickness up to 50 nm. Moreover, efficiency of CIGS solar cells with a Ga content of approximately 0.68 was increased up to 14.8% by modifying preparation condition of ZnSe thin-films.

## 6. Conclusion

In this study, increasing efficiency of CIGS solar cell with high Ga content was attempted by experiment and numerical evaluation. As a cause of this problem, conduction band profile in CIGS with high Ga content and recombination at CdS/CIGS interface was focused on.

From result of high temperature preparation, it was found that modifying conduction band profile was not effective in an

improvement of  $V_{OC}$  drastically although FF was improved. On the other hand, formation of  $\Delta E_V$  by incorporating ZnSe at CdS/CIGS interface was effective in an improvement of  $V_{OC}$ , resulting in a  $V_{OC}$  of 0.792 V. These results agree with the result of numerical evaluation. Therefore, it is possible that an efficiency of above 22% is obtained by further understanding of the  $\Delta E_V$  effect and optimizing preparation method of ZnSe thin-films. Subsequently, it is believed an efficiency of above 25% is realized by forming the single-graded conduction band profile and reducing the defect density in the CIGS with high Ga content, using CIGS absorbers with high Ga content.

## References

- [1] I. Repins, et al., Prog. Photovol. Res. 16 (2008) 235.
- [2] <http://www.zsw-bw.de/en/support/news/news-detail/zsw-brings-world-record-back-to-stuttgart.html>
- [3] <http://www.solar-frontier.com/eng/news/2014/C031367.html>
- [4] <http://www.empa.ch/plugin/template/empa/1/131438/---/l=2>
- [5] M. A. Contreras, et al., Prog. Photovol. Res. Appl. 20 (2012) 843.
- [6] P. Jackson, et al., Prog. Photovoltaics 19 (2011) 894.
- [7] I. Repins, et al., Prog. Photovoltaics 16 (2008) 235.
- [8] N. Kohara, et al., Jpn. J. Appl. Phys. 34 (1995) L1141.
- [9] H. Miyazaki, et al., J. Phys. Chem. Solids 64 (2003) 2055.
- [10] S. H. Wei, et al. Appl. Phys. Lett. 72 (1998) 3199.
- [11] T. Minemoto, et al., J. Appl. Phys. 13 (2013) 103.
- [12] Y. Hirai, et al., Jpn. J. Appl. Phys. 51 (2012) 10NC03.
- [13] Y. Hirai, et al., Jpn. J. Appl. Phys. 53 (2014) 012301.